Journal of Physics:
Conference Series

PAPER • OPEN ACCESS

Natural Frequency and Thermal Buckling Behaviour of Delaminated Composite Plate

To cite this article: M Sayed *et al* 2025 *J. Phys.: Conf. Ser.* **3058** 012001

Natural Frequency and Thermal Buckling Behaviour of Delaminated Composite Plate

M Sayed[1], S Saleh[1] and H H Ibrahim[2]

[1] Aerospace Engineering, Military Technical College, Cairo, 11766, Egypt.
[2] Mechatronics Engineering, German University in Cairo, 11835, Egypt.
E-mail: eng.msayedhasan@gmail.com

Abstract. Delamination is a critical damage mechanism in laminated composites that significantly reduces structural stiffness, leading to adverse effects on dynamic behaviour. This study investigates the impact of delamination on the natural frequency of moderately thin composite panels using a nonlinear finite element model. The model is developed based on first-order shear deformation theory, von Karman strain-displacement relations, and the principle of virtual work to capture the dynamic response of delaminated panels accurately. The delaminated region is modelled using an effective stiffness approach, which adjusts the local stiffness properties to reflect the degradation due to damage. The proposed model provides robust thermomechanical property estimates for delaminated composites, enabling precise evaluation of the shifts in natural frequency under thermal and mechanical loading. Numerical simulations demonstrate the influence of delamination length, location on the natural frequency, offering insights into the sensitivity of composite structures to delamination-induced degradation. This study contributes to improved predictive capabilities for the dynamic performance of damaged composite structures, supporting the development of more resilient and reliable composite materials.

1. Introduction

The natural frequency of composite laminates is a critical parameter in assessing their dynamic performance, as it directly influences the material's vibrational response and stability under operational conditions. Anderson and Nayfeh [1] investigated the natural frequencies and mode shapes of laminated composite plates, comparing experimental results with finite element analysis (FEA) to validate predictive accuracy and enhance understanding of composite behaviour.

Zhuo et al. [2] explored the nonlinear vibrations of Fiber metal laminate thin plates, accounting for both geometric and material nonlinearities through theoretical analysis and experimental validation. Yildiz et al. [3] studied free vibration analyses of 3D-printed plates with various geometric infills, combining experimental testing with numerical simulations to assess the impact of internal structures on vibrational behaviour. Pishvar et al. [4] examined the damping behaviour of active composite plates with random fiber orientations and embedded unidirectional shape memory alloy (SMA) wires, highlighting how SMA integration enhances damping performance and control in composite structures.

Elevated temperatures can significantly affect the natural frequency of composite laminates by altering stiffness and geometric configuration, which can lead to thermal buckling and impact the dynamic stability and performance of the structure. Kumar [5] presented a detailed study on the vibration and buckling behaviour of advanced composite plates using a closed-form dynamic stiffness formulation, providing an analytical framework for predicting the dynamic response and stability limits of composite structures. Ibrahim et al. [6] investigated the thermal buckling behaviour of functionally graded material (FGM) panels and shape memory alloy hybrid composite panels, utilizing the first-order shear deformation theory (FSDT) and nonlinear finite element method (FEM). Shiau et al. [7] investigated the thermal buckling behaviour of composite laminated plates, focusing on how temperature variations affect the stability and performance of these structures under thermal loading conditions. Ibrahim and Tawfik [8] examined how adding shape memory alloys (SMAs) impacts thermal buckling in composite plates, finding that SMAs enhance stability under high temperatures. Ibrahim et al. [9] studied thermal buckling in shape memory alloy (SMA) hybrid composite shells, assessing the impact of SMA integration on stability under thermal loads.

Salhi et al. [10] investigated how temperature variations impact the vibration behaviour of laminated composite plates, revealing that elevated temperatures can significantly alter stiffness and natural frequencies, thereby affecting overall structural performance. Yang et al. [11] studied the dynamic degradation behaviours of ceramic matrix composite thin plates under extremely high-temperature conditions, using both theoretical and experimental approaches to demonstrate how severe thermal environments accelerate degradation, impacting the material's vibrational and structural integrity. Zhao et al. [12] examined how temperature variations affect the modal characteristics of composite honeycomb structures, using experimental and simulation methods to show that temperature changes significantly influence natural frequencies and dynamic responses.

Delamination caused by matrix cracking significantly affects the natural frequency of composite laminates, with elevated temperatures further reducing stiffness, affecting thermal expansion of temperature dependant materials and altering dynamic behaviour, potentially compromising structural performance. Della and Shu [13] provided a detailed examination of how delamination impacts the vibrational characteristics of composite laminates, an essential consideration for maintaining structural performance in advanced engineering applications. H. Chen et al. [14] explored the impact of nonlinear contact on the natural frequency of delaminated stiffened composite plates, using finite element modelling to simulate interactions within delaminated regions. T. Mukhopadhyay et al. [15] studied the effects of delamination on the stochastic natural frequencies of composite laminates, using a probabilistic approach to analyse frequency variability due to material uncertainties.

Valdes and Soutis [16] examined delamination detection in composites by analysing modal characteristics, revealing that delamination-induced stiffness reduction causes frequency shifts and mode shape changes, which serve as damage indicators. Kumar and Sarathchandra [17] investigated the effect of delamination on natural frequencies in Fiber Reinforced Polymer plates, showing through finite element analysis that delamination, especially larger or central, reduces frequencies due to localized stiffness loss. Tenek et al. [18] studied the vibration behaviour of delaminated composite plates to support non-destructive testing, demonstrating that changes in frequencies and mode shapes can effectively indicate delamination. Farrokhabadi et al. [19] developed an energy-based analytical model based on classical lamination theory, defining discrete zones within the unit cell along delamination cracks through a crack closure method.

There is a gap in research regarding the effect of elevated temperature on the natural frequency of delaminated composite laminates. Investigating this relationship offers a valuable perspective, shedding light on how temperature and delamination interact to affect the dynamic behaviour and stability of composite structures under various loading conditions. This research employs sophisticated structural analysis techniques by implementing an effective stiffness model to simulate delamination resulting from matrix crack in composite laminates. The study utilizes finite element analysis based on first-order shear deformation theory and von Kármán strain-displacement relations to represent composite laminates with pre-existing delaminated zone, thereby improving the comprehension of delamination effects. In addition, the investigation includes the analysis of thermal buckling and natural frequency, performing a comparative study between intact laminates and those exhibiting delamination to determine their structural properties. This research assesses how changes in delamination length, location, and ply orientation affect the dynamic response under thermal conditions aiming to bridge existing gaps in understanding by providing a detailed examination of temperature effects on delaminated laminates, with implications for design optimization in thermally demanding applications.

2. Methodology

2.1. Modeling of Delaminated Composites

An elastic composite laminate subjected to mechanical or thermal stresses can develop delamination, making it crucial to investigate this failure mode to maintain the structural integrity and long-term performance of composite materials in challenging environments.

Once a delamination onset, the transfer of stress between adjacent plies is interrupted, resulting in a reduction of the laminate's stiffness and potentially leading to structural failure. The elastic constants are employed to describe the stress-strain behaviour of anisotropic materials and are calculated using the equation for the reduced stiffness matrix of an orthotropic ply in local coordinates, following the principles of Classical Lamination Theory. The reduced stiffness for each lamina, along with its thermal expansion properties, is transformed from local to global coordinates, enabling the calculation of the extensional, coupling, and bending stiffness matrices.

When a pre-existing crack exists in any ply, an Effective Stiffness Model is employed, based on the framework outlined in reference [20]. This model assists in evaluating the mechanical properties and the decrease in stiffness of the damaged lamina resulting from delamination at the interfaces between the plies.

The laminate is divided into two distinct regions: an undamaged region and a fully delaminated region. This segmentation is essential for accurately calculating the overall stiffness of the laminate matrix, taking into account the presence of cracks.

Figure 1. Damaged ply in composite laminate

The compliance matrix of each ply $\left(\bar{a}_{ij}\right)_k$ of thickness h_k and reduced stiffness matrix of $\left[\bar{Q}_{ij}\right]_k$ is obtained using the following equation:

$$\left(\bar{a}_{ij}\right)_k = \left(\frac{\left[\bar{Q}_{ij}\right]_k * h_k}{h}\right)^{-1} \tag{1}$$

By using the compliance matrices of the 0° and 90° plies in a symmetric cross laminate with thicknesses of h_0 and h_{90}, respectively, the compliance matrix for the fully delaminated zone can be derived, as detailed below:

$$\begin{bmatrix} a_{11}^{del} & a_{12}^{del} & a_{13}^{del} \\ a_{21}^{del} & a_{22}^{del} & a_{23}^{del} \\ a_{31}^{del} & a_{32}^{del} & a_{33}^{del} \end{bmatrix} = \begin{bmatrix} a_{11}^{0}\dfrac{h}{h_0} & a_{12}^{0} & a_{13}^{0}\dfrac{h}{h_0} \\ a_{21}^{0} & a_{22}^{0}\dfrac{h_0}{h} + a_{22}^{90}\dfrac{h_{90}}{h} & a_{23}^{0} \\ a_{31}^{0}\dfrac{h}{h_0} & a_{32}^{0} & a_{33}^{0}\dfrac{h}{h_0} \end{bmatrix} \tag{2}$$

Furthermore, in the delaminated zone, the thermal expansion of the lamina is affected by the following equation:

$$\begin{bmatrix}\alpha_x^{del}\\ \alpha_y^{del}\\ \alpha_s^{del}\end{bmatrix}=\begin{bmatrix}\alpha_x^0\\ \alpha_y^0\dfrac{h_{90}}{h}+\alpha_y^0\dfrac{h_{90}}{h}\\ \alpha_s^0\end{bmatrix} \tag{3}$$

The overall laminate compliance matrix a_{ij} and thermal expansion α can be represented as follows:

$$a_{ij}=(1-\eta)a_{ij}^{o}+\eta a_{ij}^{del} \tag{4}$$

$$\alpha=(1-\eta)\alpha^{o}+\eta\alpha^{del} \tag{5}$$

Where; η is the ratio between delaminated length to total length. The damaged stiffness matrix is determined using the following equation:

$$A_{ij}^{dam}=\left[a_{ij}\right]^{-1}=\sum Q_k h_k \tag{6}$$

Delamination in the 90° ply is the cause of the laminate's decreased stiffness matrix. As a result, that ply's altered stiffness matrix is first identified in the global coordinate system and then converted into the local coordinate system. This procedure aids in defining the mechanical property reduction at a given delamination length.

$$\bar{Q}_{90}^{dam}=\frac{1}{2h_{90}}\left(A_{ij}^{dam}-2\bar{Q}_0h_0\right) \tag{7}$$

When there is a pre-existing crack in one or more plies of the laminate, the damaged ply which has a lower stiffness matrix because of delamination is replaced out with an undamaged ply with lower mechanical properties. The Classical Laminate Theory (CLT) is used to find the ABD matrices in order to do this replacement and examine the behaviour of the laminate.

$$A_{ij}=\sum_{k=1}^{n}\int_{Z_{k+1}}^{Z_k}\left[Q_{ij}\right]_k dz \tag{8}$$

$$B_{ij}=\frac{1}{2}\sum_{k=1}^{n}\int_{Z_{k+1}}^{Z_k}\left[Q_{ij}\right]_k zdz \tag{9}$$

$$D_{ij}=\frac{1}{3}\sum_{k=1}^{n}\int_{Z_{k+1}}^{Z_k}\left[Q_{ij}\right]_k z^2dz \tag{10}$$

The compliance matrix of the laminate [S] can be expressed from the following equations, which will be utilized to ascertain the mechanical properties of the laminate:

$$A^{*}=A^{-1} \tag{11}$$

$$B^{*}=A^{-1}B \tag{12}$$

$$C^{*}=BA^{-1} \tag{13}$$

$$D^{*}=D-BA^{-1}B \tag{14}$$

$$S=\begin{bmatrix}A^{*} & B^{*}\\ C^{*} & D^{*}\end{bmatrix}^{-1} \tag{15}$$

Using the damaged laminate compliance matrix obtained, we can determine the mechanical properties of the damaged laminate at different delamination length delamination as follows:

$$E_x(\eta) = \frac{1}{S_{(1,1)}} \quad (16)$$

$$E_y(\eta) = \frac{1}{S_{(2,2)}} \quad (17)$$

$$\nu_{xy}(\eta) = \frac{-E_x}{S_{(1,2)}} \quad (18)$$

$$G_{xy}(\eta) = \frac{1}{S_{(6,6)}} \quad (19)$$

With the ABD matrices defined, characterizing the composite panel's stiffness under in-plane and bending loads, we proceed to finite element modelling. These matrices are incorporated into the element properties, enabling detailed analysis of the panel's structural behaviour under loading.

2.2. Deriving the Equation of Motion

In this section, we present the finite element modelling approach and the systematic methodology used to derive the equation of motion. The panel strain is assumed to follow the first order shear deformation theory, while the nonlinear deflections are supposed to follow the von Karman strain displacement relations.

A four-node element is utilized, incorporating four transverse degrees of freedom and two in-plane degrees of freedom per node to accurately represent both bending and in-plane behaviours within the model.

$$\{\delta\} = \{w, \frac{\partial w}{\partial x}, \frac{\partial w}{\partial y}, \frac{\partial^2 w}{\partial x \partial y}, u, v\}^T = \{w_b, w_m\}^T \quad (20)$$

Where; w_b is the out of plane deflections and w_m is in-plane deflections.

The von Kármán large deflection theory models the nonlinear behaviour of thin elastic plates under large deformations, where deflections are comparable to the plate thickness.

$$\epsilon^o = \begin{Bmatrix} \frac{\partial u}{\partial x} \\ \frac{\partial v}{\partial y} \\ \frac{\partial u}{\partial y} + \frac{\partial v}{\partial x} \end{Bmatrix} \quad (21)$$

$$\kappa = \begin{Bmatrix} -\frac{\partial^2 w}{\partial x^2} \\ -\frac{\partial^2 w}{\partial y^2} \\ -2\frac{\partial^2 w}{\partial x \partial y} \end{Bmatrix} \quad (22)$$

Where; κ is bending curvature vector and $\{\epsilon^o\}$ is total strain.

The resultant force and moment vectors per unit length are defined as:

$$\begin{bmatrix} N \\ M \end{bmatrix} = \begin{bmatrix} A & B \\ B & D \end{bmatrix} \begin{bmatrix} \epsilon^o \\ \kappa \end{bmatrix} - \begin{bmatrix} N_T \\ M_T \end{bmatrix} \quad (23)$$

Based on the reduced stiffness matrix and thermal expansion of each ply, the thermal force and moment delivered to the laminate can be calculated as follows:

$$N_T = \sum_{k=1}^{n} \int_{Z_{k+1}}^{Z_k} [Q_{ij}]_k \int_{T_ref}^{T} \left(\begin{bmatrix} \alpha_x(T) \\ \alpha_y(T) \\ \alpha_{xy}(T) \end{bmatrix}^k \right) dTdZ \tag{24}$$

$$M_T = \sum_{k=1}^{n} \int_{Z_{k+1}}^{Z_k} [Q_{ij}]_k \int_{T_ref}^{T} \left(\begin{bmatrix} \alpha_x(T) \\ \alpha_y(T) \\ \alpha_{xy}(T) \end{bmatrix}^k \right) dTzdZ \tag{25}$$

The governing equations are derived using the principle of virtual work which is widely applied in mechanics to establish equations of motion. For a plate element, the virtual work from internal forces includes contributions from bending moments, shear forces, and membrane forces, acting through virtual displacements related to bending, twisting, and in-plane deformations. This is obtained by integrating the product of internal stresses and virtual strains over the plate surface, expressed as follows:

$$\delta W = \delta W_{int} - \delta W_{ext} = 0 \tag{26}$$

$$\delta W_{\text{int}} = \int_A (\{\delta\varepsilon^\circ\}^T\{N\} + \{\delta\kappa\}^T\{M\})\, dA \tag{27}$$

$$\delta W_{int} = \begin{Bmatrix} \delta w_b \\ \delta w_m \end{Bmatrix}^T \left(\begin{bmatrix} k_b & k_{bm} \\ k_{mb} & k_m \end{bmatrix} - \begin{bmatrix} k_{Tb} & 0 \\ 0 & 0 \end{bmatrix} + \frac{1}{2} \begin{bmatrix} n_{1b} & n_{lbm} \\ n_{1mb} & 0 \end{bmatrix} + \frac{1}{3} \begin{bmatrix} n_{2b} & 0 \\ 0 & 0 \end{bmatrix} \right) \begin{Bmatrix} w_b \\ w_m \end{Bmatrix} - \begin{Bmatrix} \delta w_b \\ \delta w_m \end{Bmatrix}^T \begin{Bmatrix} p_{bT} \\ p_{mT} \end{Bmatrix} \tag{28}$$

When considering inertia and aerodynamics, the virtual work that external forces do on a panel element is as follows:

$$\delta W_{ext} = - \begin{Bmatrix} \delta w_b \\ \delta w_m \end{Bmatrix}^T \begin{bmatrix} m_b & 0 \\ 0 & m_m \end{bmatrix} \begin{Bmatrix} \ddot{w}_b \\ \ddot{w}_m \end{Bmatrix} - \begin{Bmatrix} \delta w_b \\ \delta w_m \end{Bmatrix}^T \begin{bmatrix} g & 0 \\ 0 & 0 \end{bmatrix} \begin{Bmatrix} \dot{w}_b \\ \dot{w}_m \end{Bmatrix} - \begin{Bmatrix} \delta w_b \\ \delta w_m \end{Bmatrix}^T \lambda \begin{bmatrix} a_a & 0 \\ 0 & 0 \end{bmatrix} \begin{Bmatrix} w_b \\ w_m \end{Bmatrix} \tag{29}$$

k_b , k_{bm} , k_{mb} , k_m represent the elementary linear stiffness matrices. k_{Tb} represents elementary thermal stiffness matrix. n_{1b} , n_{2b} , n_{bm} , n_{mb} represent the elementary nonlinear stiffness matrices. p_{bt} , p_{mt} are elementary bending and membrane thermal forces vectors. m_b , m_m represent the elementary mass matrices. a_a and g are elementary aerodynamic stiffness matrix and aerodynamic damping matrix respectively. A is area of the element.

The element equation of motion is expressed as:

$$\{\ddot{w}\} + [g]\{\dot{w}\} + \left(\lambda[a_a] + [k] - [k_T] + \frac{1}{2}[n_1] + \frac{1}{3}[n_2]\right)\{w\} = \{p_T\} \tag{30}$$

Where; $[n_1]$ and $[n_2]$ are first and second order nonlinear stiffness matrices.

The element equations of motion are assembled to the system level, boundary conditions are applied, and the contributions from each element are combined to produce the system equations of motion, which are as follows:

$$\{\ddot{W}\} + [G]\{\dot{W}\} + \left(\lambda[A_a] + [K] - [K_T] + \frac{1}{2}[N_1] + \frac{1}{3}[N_2]\right)\{W\} = \{P_T\} \tag{31}$$

With the equation of motion derived, capturing the dynamic response of the panel under external forces, we can now analyse critical performance metrics, such as thermal buckling and natural frequency. These parameters are obtained by solving the equation of motion under thermal loading conditions and by examining the system's vibrational characteristics, respectively, providing insight into stability and resonance behaviour.

2.3. Thermal Buckling and Natural Frequency

This section derives the governing equations for thermal buckling and natural frequency in moderately thin composite plates using First-Order Shear Deformation Theory (FSDT) and Von Kármán strain-displacement relations to determine critical buckling temperature and post-buckling response.

By simplifying the equation of motion—omitting the mass, aerodynamic stiffness, and damping matrices—the Newton-Raphson method is employed to solve iteratively for convergence.

$$\left([K]-[K_T]+\frac{1}{2}[N_1]+\frac{1}{3}[N_2]\right)\{W\}=\{P_T\} \tag{32}$$

Introducing the function $\{\Psi(W)\}$ the equation will be:

$$\{\Psi(W)\}=\left([K]-[K_T]+\frac{1}{2}[N_1]+\frac{1}{3}[N_2]\right)\{W\}-\{P_T\}=0 \tag{33}$$

It can be expressed as follows in the form of a shortened Taylor series expansion:

$$\{\Psi(W+\delta W)\}=\{\Psi(W)\}+\frac{d\{\Psi(W)\}}{d(W)}\{\Psi(\delta W)\}\approx 0 \tag{34}$$

$$\frac{d\{\Psi(W)\}}{d(W)}=\left([K]-[K_T]+\frac{1}{2}[N_1]+\frac{1}{3}[N_2]\right)=[K_{tan}] \tag{35}$$

Newton-Raphson technique is applied to obtain post buckling behaviour:

$$\{\Psi(W)\}_i=\left([K]-[K_T]+\frac{1}{2}[N_1]_i+\frac{1}{3}[N_2]_i\right)\{W\}-\{P_T\}=0 \tag{36}$$

$$\{\delta(W)\}_{i+1}=-[K_{tan}]^{-1}\{\Psi(W)\}_i \tag{37}$$

$$\{\Psi(W)\}_{i+1}=\{\Psi(W)\}_i+\{\delta(W)\}_{i+1} \tag{38}$$

Convergence is achieved in this process when the maximum value of $\{\delta(W)\}_{i+1}$ falls below a defined tolerance, ϵ_{tol}

Understanding the natural frequency of a structure following thermal buckling is essential, as it reveals how temperature variations can impact vibrational characteristics and potentially lead to failure under dynamic loading conditions.

The differential equation of motion can be solved by adding the time-dependent homogeneous solution and the time-independent specific solution.

$$[M]\{\ddot{W}\}+[G]\{\dot{W}\}+\left(\lambda[A_a]+[K]-[K_T]+\frac{1}{2}[N_1]+\frac{1}{3}[N_2]\right)\{W\}=\{P_T\} \tag{39}$$

$$\{W\}=\{W\}_s+\{W\}_t \tag{40}$$

The linear vibration frequency of the plate about the equilibrium position can be found once the plate buckling equilibrium position Ws for a given temperature rise ΔT is established.

The thermal load vector P_T is independent on time. W_s is the aero-thermal static equilibrium deflection, which is the particular. while Wt is a self-excited dynamic oscillation, which is the homogeneous solution.

$$\begin{gathered}[M]\left(\{\ddot{W}_s\}+\{\ddot{W}_t\}\right)+[G]\left(\{\dot{W}_s\}+\{\dot{W}_t\}\right)\\+\left(\lambda[A_a]+[K]-[K_T]+\frac{1}{2}[N_1]_{s+t}+\frac{1}{3}[N_2]_{s+t}\right)(\{W_s\}+\{W_t\})=\{P_T\}\end{gathered} \tag{41}$$

$$[N_1]_{s+t}=[N_1]_s+[N_1]_t \tag{42}$$

$$[N_2]_{s+t}=[N_2]_s+2[N_2]_{st}+[N_2]_t \tag{43}$$

$$[M]\{\ddot{W}\}_t + [G]\{\dot{W}\}_t + \left(\lambda[A_a] + [K] - [K_T] + \frac{1}{2}[N_1]_t + \frac{1}{3}[N_2]_t\right)\{W\}_t + \left(\frac{1}{2}[N_1]_t + \frac{1}{3}[N_2]_t + \frac{2}{3}[N_2]_{st}\right)\{W\}_s + \left(\frac{1}{2}[N_1]_s + \frac{1}{3}[N_2]_s + \frac{2}{3}[N_2]_{st}\right)\{W\}_t = 0 \quad (44)$$

Following the derivation in [9] the nonlinear differential equations will be:

$$[M]\{\ddot{W}\}_t + [G]\{\dot{W}\}_t + \left(\lambda[A_a] + [K] - [K_T] + \frac{1}{2}[N_1]_t + \frac{1}{3}[N_2]_t\right)\{W\}_t + ([N_1]_s + [N_2]_s + [N_2]_{st})\{W\}_t = 0 \quad (45)$$

By dropping the damping matrices, aerodynamic stiffness, and the nonlinear stiffness matrices which depend on the time-dependent displacement $\{W\}_t$, the free vibration equation will be:

$$[M]\{\ddot{W}\}_t + ([K] - [K_T] + [N_1]_s + [N_2]_s)\{W\}_t = 0 \quad (46)$$

$$\{\ddot{W}\}_t + [K_{tan}]\{W\}_t = 0 \quad (47)$$

Assuming the solution of the equation in harmonic form:

$$\{W\}_t = \bar{c}\{\Phi\}e^{\Omega t} \quad (48)$$

The eigenvalue problem will be:

$$(\Omega^2[M] + [K_{tan}])\{\Phi\} = 0 \quad (49)$$

Solving this eigenvalue problem, the free vibration of a thermally buckled composite panel will be obtained.

3. Results

This work provides a thorough modeling method for a symmetric composite laminate with a plate size of 0.308 m x 0.3 m, a total thickness of 0.0013 m, and a symmetric stacking sequence of [0 -45 45 90] as shown in figure 2.

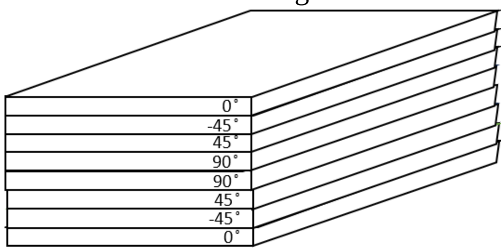

Figure 2. Undamaged Laminate

Symbol	Value
E_1	155 (1-6.35x10^{-4} ΔT) GPa
E_2	8.07 (1-7.69x10^{-4} ΔT) GPa
G_{12}	4.55(1-1.09x10^{-3}ΔT) GPa
ρ	1550 Kg/m^3
ν	0.22
α_1	-0.07x10^{-6}(1-0.69x10^{-3}ΔT) / ºC
α_2	30.6x10^{-6}(1+0.28x10^{-4}ΔT) / ºC

Table 1. Material properties of Graphite-Epoxy composite lamina

3.1. Mechanical Properties Degradation

The model is used to measure the reduction in the composite laminate's mechanical properties that results from pre-existing cracks in different plies at predetermined delamination lengths.

The variations in the normalized longitudinal modulus of elasticity (E_x) and the normalized transverse modulus of elasticity (E_y) with increasing delamination length are illustrated in figures 3 and 4, focusing on delamination across different plies. As anticipated, the results reveal that delamination in the -45° and 45° plies leads to equivalent reductions in longitudinal and transverse stiffness, with these decreases being less pronounced than those seen in other orientations. The most significant reduction in longitudinal stiffness is observed with delamination in the 0° plies, while the greatest decrease in transverse stiffness occurs in the 90° plies.

The impact of increasing delamination length on the modulus of rigidity of the composite laminate is presented in figure 5. As expected, the initiation of matrix cracks in either the 0° or 90° plies leads to a similar reduction in the in-plane shear modulus as delamination length increases. In addition, the decrease in the in-plane shear modulus remains consistent regardless of whether the matrix crack occurs in the -45° or 45° plies. Furthermore, when comparing damage scenarios in the 0° or 90° plies, laminates exhibit a significantly smaller reduction in the in-plane shear modulus if the matrix crack initiates in the -45° or 45° plies.

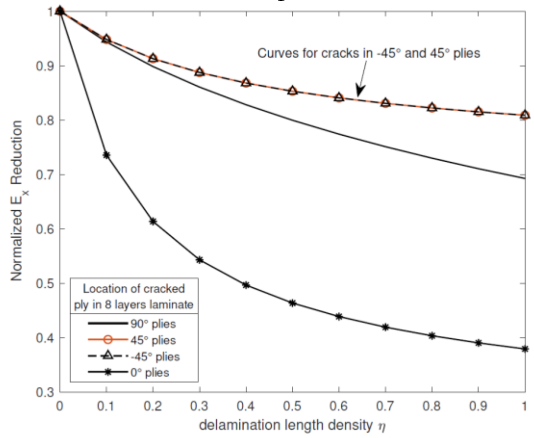

Figure 3. Longitudinal modulus of elasticity.

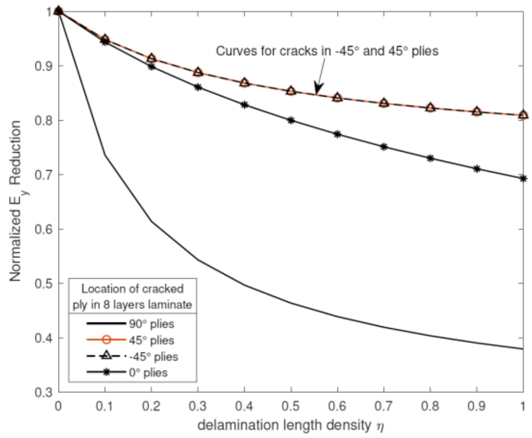

Figure 4. Transverse modulus of elasticity.

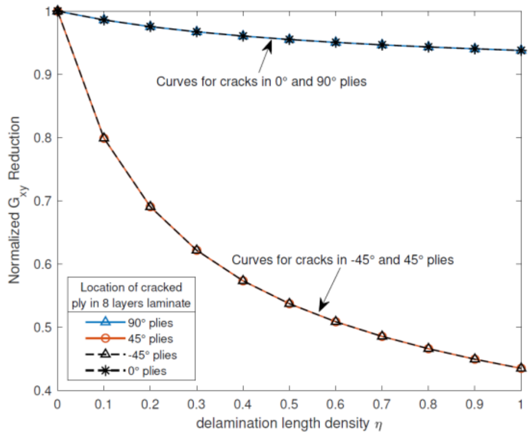

Figure 5. Rigidity modulus.

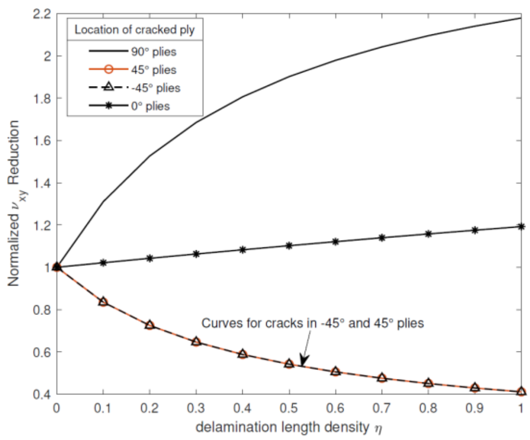

Figure 6. Poison ratio.

The changes in Poisson's ratio due to delamination growth are illustrated in figure 6. It is observed that the normalized Poisson's ratio is less affected when delamination occurs in the outer plies, and the reduction remains equivalent when damage is present in the 45° and -45° plies. In contrast, notable changes in Poisson’s ratio are evident when delamination occurs in the 90° plies or in plies near the midplane.

3.2. Thermal Buckling

This section presents the results of analysis on thermal buckling for simply supported fixation, detailing the critical temperatures and post buckling behaviour of both undamaged laminates and those with delamination lengths of 0.2, 0.5, and 0.7.

The findings were surprising, as the presence of delamination resulted in a reduction of stiffness but did not lead to a decrease in the critical buckling temperature. Instead, delamination appears to alter the thermal buckling behaviour of the laminate, primarily due to the effects of thermal expansion. Both the location of the crack and the length of the delaminated region significantly influence the critical buckling temperature and post-buckling behaviour. The highest critical buckling temperature is recorded in instances where the crack is situated in the outer plies, particularly with a delamination length of 0.5, as illustrated in figure 7.

The post-buckling behaviour of cracks oriented at -45° and 45°, as shown in figures 8 and 9, reveals similarities for delamination lengths of 0.2 and 0.7. the behaviour remains similar when delamination occurs in the midplane plies as shown in figure 10 with a higher critical buckling temperature for the case of delamination length of 0.7.

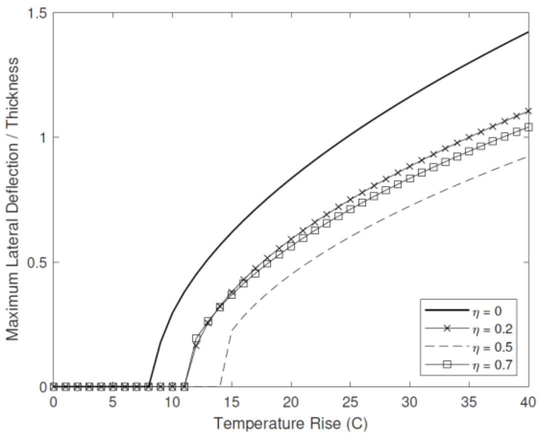

Figure 7. Crack in 0° plies.

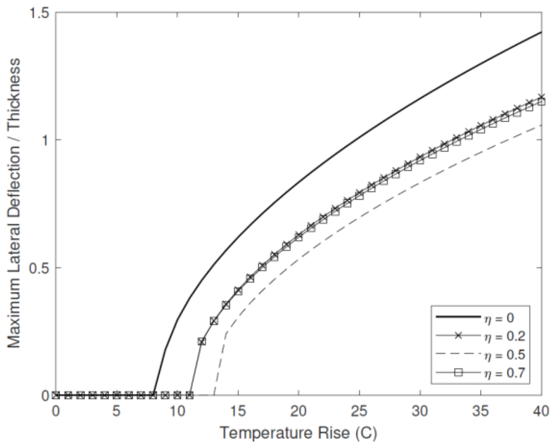

Figure 8. Crack in -45° plies.

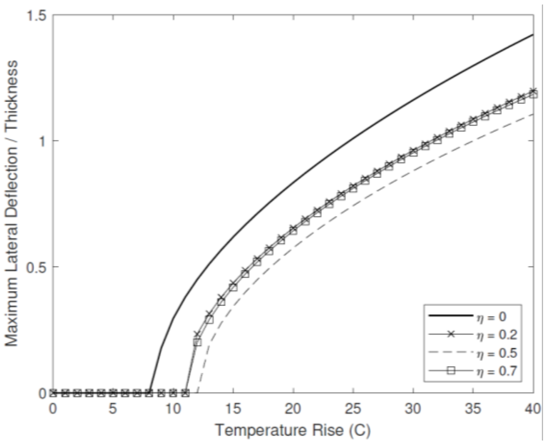

Figure 9. Crack in 45° plies.

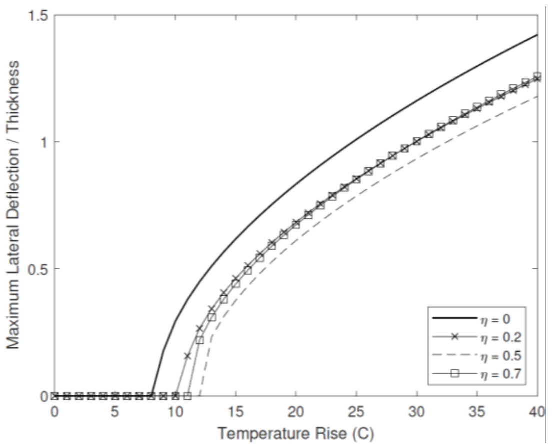

Figure 10. Crack in 90° plies.

When a delamination length of 0.5 is considered, the impact of delamination becomes less significant if it occurs within the midplane plies, as indicated in figure 10. This observation suggests that the midplane layers display greater resistance to the adverse effects of delamination compared to the outer plies. This increased resistance can be attributed to their central location within the laminate stack, which contributes to a more uniform stress distribution across the thickness of the composite laminate. As a result, the mechanical integrity of the laminate is better preserved when delamination occurs in these midplane regions. Thus, understanding the relationship between delamination characteristics and thermal buckling behaviour is crucial for improving the design and reliability of composite materials under thermal loads.

3.3. Natural Frequency

This section presents the findings on the natural frequency of simply supported panels under elevated temperatures, focusing on both undamaged and damaged conditions with delamination lengths of 0.2, 0.5, and 0.7.

The behaviour of natural frequency in simply supported panels subjected to elevated temperatures indicates that, as the temperature increases, the natural frequency decreases due to stiffness degradation up to the critical buckling temperature. Beyond this threshold, for buckled panels, the natural frequency begins to increase with further temperature rise, likely due to changes in the structural dynamics and energy dissipation mechanisms. This transition reflects the complex interplay between thermal effects and the mechanical properties of the composite laminate.

The effect of delamination on buckled composite panels at temperatures exceeding the critical buckling temperature is significantly more pronounced than on flat panels. Notably, when cracks are present in the 0° plies, as shown in figure 11, the impact on panel performance is greater compared to other ply orientations. Conversely, the effect is minimal when delamination occurs in the 90° plies at the midplane, as indicated in figure 14. This variation in sensitivity highlights the importance of ply orientation in assessing the structural integrity and dynamic behaviour of delaminated composite materials under load.

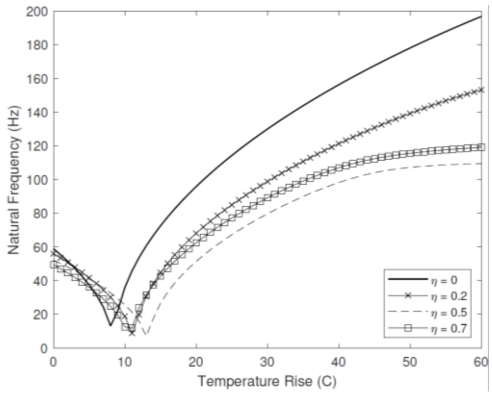

Figure 11. Crack in 0° plies.

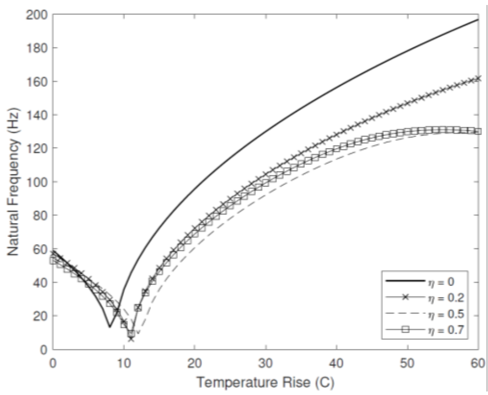

Figure 12. Crack in -45° plies.

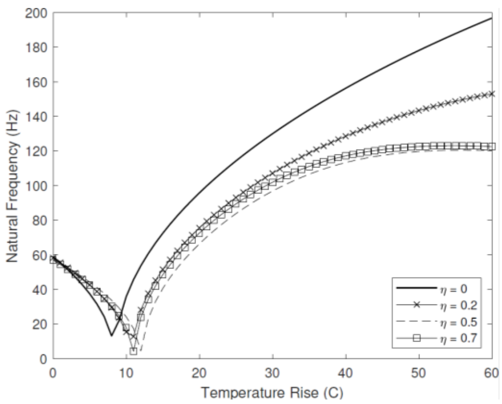

Figure 13. Crack in 45° plies.

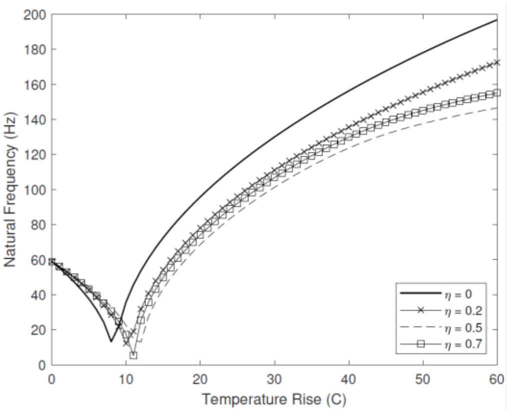

Figure 14. Crack in 90° plies.

The behaviour of natural frequency under buckling conditions shows similar effects when the crack is present in either the -45° or 45° plies as illustrated in figures 12 and 13. This indicates that both orientations exhibit comparable sensitivity to delamination, impacting the overall dynamic response of the composite panels similarly. Understanding these patterns is essential for predicting structural performance and ensuring the reliability of composite materials in engineering applications.

4. Conclusion

This study examines the effects of elevated temperature on the natural frequency of simply supported composite panels, considering both undamaged and delaminated configurations. It also explores how varying delamination length, orientation, and location influence mechanical properties, thermal buckling behaviour, and dynamic response. The findings offer critical insights into the stability and performance of composite panels subjected to thermal loading.

The investigation reveals that natural frequency decreases as temperature rises toward the critical buckling temperature, primarily due to a loss in stiffness associated with thermal effects. This reduction in stiffness lowers the panel's resistance to dynamic forces, leading to a drop in natural frequency. However, once the buckling threshold is reached, the panel exhibits nonlinear behaviour, where the effects of the nonlinear stiffness matrices cause an increase in natural frequency with further temperature rise, reflecting changes in post-buckling stiffness.

Delamination significantly impacts the mechanical properties of composite panels, particularly under buckled conditions. Panels with delamination at 0° plies experience the greatest reduction in natural frequency and stiffness, due to the primary load-bearing orientation's sensitivity to damage. The effect of delamination in ±45° plies is moderate, showing comparable patterns but less pronounced. Delamination located in the 90° plies at the midplane shows the least effect, due to reduced load transmission in this orientation.

The location of delamination further affects thermal buckling, with centrally located delamination having a greater impact on stability and frequency shifts. Larger delamination also led to more pronounced reductions in natural frequency at high temperatures, indicating that delamination extent is a key parameter for assessing structural reliability. Overall, this research highlights the critical role of ply-specific and location-specific delamination analysis in predicting and optimizing composite panel behaviour in thermally variable environments.

5. References

[1] Anderson T J and Nayfeh A H 1996 Natural frequencies and mode shapes of laminated composite plates: experiments and FEA *Journal of Vibration and Control* **2** 381–414

[2] Zhuo X, Chen C, Hui L, Da-Wei G, Xian-Chao S, Chang-cheng H, He L, Qing-kai H and Bang-chun W 2024 Nonlinear vibrations of fiber metal laminates thin plates considering both geometric and material nonlinearity: Theoretical and experimental *International Journal of Structural Stability and Dynamics*

[3] Yildiz A, \.Ibram E, Erol O and Güler Özgül H 2024 Zeitschrift für Naturforschung: Free vibration analyses of 3D printed plates with different geometric fillings: experimental testing and numerical simulations

[4] Pishvar M, Padilla A and Bishay P L Damping Behavior of Active Composite Plates with Random Fiber Orientation and Embedded Unidirectional Shape Memory Alloy Wires *Available at SSRN 4974251*

[5] Kumar R 2024 *Vibration and Buckling Analysis of Advanced Composite Plates Using Closed-Form Dynamic Stiffness Formulation* (IIT Kharagpur)

[6] Ibrahim H H, Yoo H H and Lee K-S 2009 Aero-thermo-mechanical characteristics of imperfect shape memory alloy hybrid composite panels *J Sound Vib* **325** 583–96

[7] Shiau L-C, Kuo S-Y and Chen C-Y 2010 Thermal buckling behavior of composite laminated plates *Compos Struct* **92** 508–14
[8] Ibrahim H H, Tawfik M and Negm H M 2011 Thermal buckling and nonlinear flutter behavior of shape memory alloy hybrid composite plates *Journal of Vibration and Control* **17** 321–33
[9] Ibrahim H H, Yoo H H and Lee K-S 2009 Thermal buckling and flutter behavior of shape memory alloy hybrid composite shells *J Aircr* **46** 895–902
[10] Salhi M L, Mellas M and Ounis H 2024 The effect of temperature on the vibration behaviour of laminated composite plates
[11] Yang Y, Li H, Hou J, Sun G, Wang H, Zhang H, Wang X, Sun W, Luo Z and Han Q Dynamic Degradation Behaviors of Ceramic Matrix Composite Thin Plates with an Extremely High-Temperature Environment: Theoretical and Experimental Investigation *Available at SSRN 4935632*
[12] Bai Y, Yu K, Zhao J and Zhao R 2018 Experimental and simulation investigation of temperature effects on modal characteristics of composite honeycomb structure *Compos Struct* **201** 816–27
[13] Della C N and Shu D 2007 Vibration of delaminated composite laminates: A review *Appl Mech Rev* **60** 1–20
[14] Chen H, Wang M and Bai R 2006 The effect of nonlinear contact upon natural frequency of delaminated stiffened composite plate *Compos Struct* **76** 28–33
[15] Mukhopadhyay T, Naskar S, Karsh P K, Dey S and You Z 2018 Effect of delamination on the stochastic natural frequencies of composite laminates *Compos B Eng* **154** 242–56
[16] Valdes S H D and Soutis C 1999 Delamination detection in composite laminates from variations of their modal characteristics *J Sound Vib* **228** 1–9
[17] Kumar K D, Sarathchandra S B, Madhusudanprasad S M and Prasad K 2023 Effect of delamination on natural frequencies of laminated FRP composite plate *Mater Today Proc* **72** 1490–7
[18] Tenek L H, Henneke II E G and Gunzburger M D 1993 Vibration of delaminated composite plates and some applications to non-destructive testing *Compos Struct* **23** 253–62
[19] Jafari S R, Farrokhabadi A and Montesano J 2021 The effect of staggered matrix crack induced delamination growth on the mechanical properties of cross-ply laminates *Compos Struct* **272** 114196
[20] Delbariani-Nejad A, Farrokhabadi A and Jafari S R 2018 An energy based approach for reliability analysis of delamination growth under mode I, mode II and mixed mode I/II loading in composite laminates *Int J Mech Sci* **145** 287–98